The Mechanical Energies of the Global Atmosphere in El Niño and La Niña Years

LIMING LI AND XUN JIANG

Department of Earth and Atmospheric Sciences, University of Houston, Houston, Texas

MOUSTAFA T. CHAHINE

Science Division, Jet Propulsion Laboratory, California Institute of Technology, Pasadena, California

JINGQIAN WANG

Department of Earth and Atmospheric Sciences, University of Houston, Houston, Texas

YUK. L. YUNG

Division of Geological and Planetary Sciences, California Institute of Technology, Pasadena, California

(Manuscript received 7 March 2011, in final form 18 July 2011)

ABSTRACT

Two meteorological reanalysis datasets are analyzed to determine the mechanical energies of the global atmosphere in the El Niño and La Niña years. The general consistency of the mean energy components between the two datasets reveals ~1%–3% increase and ~2%–3% decrease in the mean energies in the El Niño years and La Niña years, respectively. These analyses further reveal that the tropospheric temperature responds to the sea surface temperature anomaly with a time lag of two months, which leads to the varying mean atmospheric energies in the El Niño and La Niña years.

1. Introduction

The term El Niño, which refers to a basin-scale warming in the tropical Pacific Ocean, takes place at intervals of 2–7 yr. The warm event and its opposite phase cold event (La Niña) are closely related to a large-scale tropical east–west seesaw in sea surface pressure (Southern Oscillation). The so-called El Niño–Southern Oscillation (ENSO) has an important effect on the atmospheric dynamics at the global scale. The study of atmospheric energetics, which explores the distribution and conversion of different atmospheric energy components, offers a valuable perspective to characterize the general circulation and dynamics of planetary atmospheres (Peixoto and Oort 1992). The characterization of atmospheric energetics in the El Niño and La Niña years, which is conducted in this study, has the potential application to explore the atmospheric dynamics and physics of ENSO events.

The atmospheric energetics have been extensively discussed based on observations (Wiin-Nielsen 1959; Krueger et al. 1965; Peixoto and Oort 1974; Oort and Peixoto 1974, 1976; Hu et al. 2004; Li et al. 2007), numerical simulations (Steinheimer et al. 2008), and the comparison between observations and numerical simulations (Sheng and Hayashi 1990; Boer and Lambert 2008). However, little attention has been paid to atmospheric energetics associated with ENSO. Studies of ENSO energetics, which are all based on the model simulations, mainly addressed the growth of El Niño (Yamagata 1985; Hirst 1986) and the oceanic energetics (Goddard and Philander 2000) during ENSO events. Based on two reanalysis datasets, we provide a comparison of the global atmospheric energies between the El Niño years, the La Niña years, and the other years, which have not been explored in the previous studies.

Corresponding author address: Liming Li, Department of Earth and Atmospheric Sciences, University of Houston, 312 Science and Research Building 1, Rm. 312, Houston, TX 77204-5007.
E-mail: lli7@mail.uh.edu

DOI: 10.1175/JAS-D-11-072.1

2. Theoretical framework of atmospheric energetics and datasets

The study of atmospheric energetics originated from the analysis of the energy budget of an individual storm one century ago (Margules 1903). Lorenz (1955) formulated the original analysis into a modern framework of atmospheric energetics, and it is also called the Lorenz energy cycle. Lorenz's framework was almost immediately utilized by Phillips (1956) in his classic work simulating the general circulation of the atmosphere in a two-layer model. Oort (1964) reformulated Lorenz's equations of atmospheric energetics in a mixed space–time domain.

The formulation from Oort (1964) will be utilized to quantify the atmospheric energetics in the El Niño and La Niña years. We will compute the following energy components: the mean available potential energy P_M, the eddy available potential energy P_E, the mean kinetic energy K_M, and the eddy kinetic energy K_E:

$$P_M = \frac{c_p}{2}\iiint \gamma([\langle T\rangle]'')^2\rho\, dx\, dy\, dz \quad P_E = \frac{c_p}{2}\iiint \gamma\{\langle(T')^2\rangle + (\langle T\rangle^*)^2\}\rho\, dx\, dy\, dz, \tag{1}$$

$$K_M = \frac{1}{2}\iiint \{[\langle u\rangle]^2 + [\langle v\rangle]^2\}\rho\, dx\, dy\, dz \quad K_E = \frac{1}{2}\iiint \{\langle(u')^2\rangle + \langle(v')^2\rangle + (\langle u\rangle^*)^2 + (\langle v\rangle^*)^2\}\rho\, dx\, dy\, dz. \tag{2}$$

In the above equations, the variables T, u, v, and ρ are air temperature, zonal wind, meridional wind, and air density, respectively. For a variable f, the symbols $\langle f\rangle$, f', $[f]$, f^*, $\overline{f}$, and f'' represent the time average, a departure from the time average, the zonal average, a departure from the zonal average, the meridional average, and a departure from the meridional average, respectively. The parameter c_p is the specific heat at constant pressure. The stability factor γ is equal to $\Gamma_d/\{[\langle\overline{T}\rangle](\Gamma_d - [\langle\overline{\Gamma}\rangle])\}$, where Γ_d is the dry adiabatic lapse rate (i.e., g/c_p) and Γ is the lapse rate of atmosphere (i.e., $-\partial T/\partial z$). The monthly evaluation of energy components, in which the transient eddies are defined as the departure from the monthly mean, is used in this study.

Based on the theoretical framework of atmospheric energetics, we use two meteorological datasets with a horizontal spatial resolution of 2.5° × 2.5°, which came from the National Centers for Environmental Prediction–Department of Energy (NCEP–DOE) Global Reanalysis 2 (NCEP-2) and the 40-yr European Centre for Medium-Range Weather Forecasts (ECMWF) Re-Analysis (ERA-40), respectively. The time period of the NCEP-2 data is from 1979 to the present, thus spanning the satellite era. The time period for ERA-40 is from 1958 to 2001. We chose the overlap time period (i.e., 1979–2001) between the two datasets to conduct our analyses of atmospheric energetics in the El Niño and La Niña years. The two reanalysis datasets have already been introduced in related documents (Kanamitsu et al. 2002; Uppala et al. 2005; Li et al. 2007). It should be mentioned that there is one more dataset from ECMWF named ERA-Interim with a time period from 1989 to 2009. We do not include the ERA-Interim dataset in this study because of its relatively late beginning time (i.e., 1989). In addition, it is possible to get a higher spatial resolution than the basic 2.5° ERA-40 atmospheric datasets, which is used in this study, from the ERA-40 full-resolution datasets. The higher spatial resolution data will mainly affect the conversion terms of atmospheric energetics (Steinheimer et al. 2008). Comparing old estimations based on a coarse spatial resolution (Peixoto and Oort 1974) with our recent study based on a higher spatial resolution (Li et al. 2007) suggests that horizontal resolutions of data do not significantly affect the estimation of energy components in the atmosphere.

A complete cycle of atmospheric energetics also includes the conversion rates between different energy components. The evaluation of conversion rates between different energy components is closely related to the vertical velocity (Oort 1964; Peixoto and Oort 1974), a variable with poor data quality in the two datasets, NCEP-2 and ERA-40 (Kanamitsu et al. 2002; Uppala et al. 2005). In addition, our examinations suggest that estimated conversion rates are significantly different, even opposite, between the two datasets (NCEP-2 and ERA-40). Therefore, we exclude the conversion rates from this study. The exclusion of the conversion rates makes it impossible to explore a complete cycle of atmospheric energetics. Here, we focus on the energy components of global atmosphere (i.e., the available potential energies and the kinetic energies).

We use sea surface temperature (SST) averaged over the Niño-3.4 region, which covers the area of 5°S–5°N, 170°–120°W, to identify the El Niño and La Niña events between 1979 and 2001. The extended reconstructed SST data (1979–2001; Smith et al. 2008) with a spatial resolution of 2° in both latitude and longitude directions, which is provided by the Physical Sciences Division in

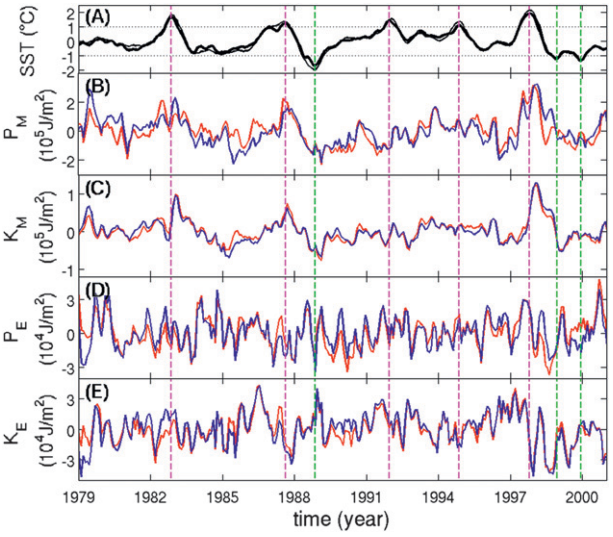

FIG. 1. Correlations between the Niño-3.4 SST index and the fluctuations of the global-average energy components. (a) The time series of the two Niño-3.4 SST indices between 1979 and 2001. Index 1 is shown by a thick black line, and index 2 is shown by a thin black line. Peaks of Niño-3.4 SST in five El Niño events (1982, 1987, 1991, 1995, and 1997) and three La Niña events (1988, 1998, and 1999) are marked by vertical dashed lines in magenta and green, respectively. The time series for the global-average energy components of (b) P_M, (c) K_M, (d) P_E, and (e) K_E. The energy components are based on NCEP-2 (red lines) and ERA-40 (blue lines) following Oort's formulation (Oort 1964; Peixoto and Oort 1974). The seasonal cycle, the mean value, and the linear trend of the energy components are removed from the time series.

the National Oceanic and Atmospheric Administration (NOAA) Earth System Research Laboratory (see online at http://www.cdc.noaa.gov/), is utilized to calculate the Niño-3.4 SST index. The calculated Niño-3.4 SST index is compared with the Niño-3.4 SST index from the Climate and Global Dynamics (CGD) Division at the University Corporation of Atmospheric Research (UCAR; see online at http://www.cgd.ucar.edu/cas/catalog/climind/Nino_3_3.4_indices.html; Trenberth 1997) in Fig. 1a. The Niño-3.4 SST indices based on the NOAA SST and from UCAR/CGD are referred as index 1 and index 2, respectively. The methodology of defining the El Niño and La Niña events in a previous study (Trenberth 1997) is used with a relatively strict criterion to emphasize the strong ENSO events. In this study, El Niño (La Niña) events are defined as three consecutive months at or above the +1.0° (at or below −1.0°) SST anomaly. Based on such a criterion, we identify five El Niño events (1982, 1987, 1991, 1995, and 1997) and three La Niña events (1988, 1998, and 1999) between 1979 and 2001. We define all other years as normal years for simplicity even though there are also some SST anomalies in these years.

3. Variation of atmospheric energies in the El Niño and La Niña years

To investigate interannual variabilities in the energy components, we remove seasonal cycles and linear trends from the time series. We also remove the mean value from the time series because we want to investigate the anomalies. After removing the seasonal cycle, the mean value, and the linear trend, we plot the time series of the global-average energy components in Fig. 1, which is compared with the Niño-3.4 SST indices. First, the two Niño-3.4 SST indices display a basic consistency. The small discrepancy between them is mainly due to the different SST data used in the two indices. Our Niño-3.4 SST index (thick line) is based on the data provided by NOAA (Smith et al. 2008), and the index from UCAR (thin line) is based on the data provided by the Hadley Centre SST dataset (Rayner et al. 2003). In addition, a general consistency of the energy components between NCEP-2 (red lines) and ERA-40 (blue lines) is seen in Figs. 1b–e. Figure 1 further suggests some correlations between the Niño-3.4 SST indices and the energy components. Correlations and maximum cross correlations between the Niño-3.4 SST index and the energy components are summarized in Table 1. The significance statistics for correlations were generated by a Monte Carlo method (Press et al. 1992) with a small numerical value of the significance level denoting a high statistical significance. A distribution of correlations was first generated by determining the correlations of three thousand isospectral surrogate time series with the relevant indices. The mean value for this distribution is zero because the correlation coefficient is zero between two random time series. The distribution of correlations was then transformed into an approximately normal distribution by the Fisher transformation (Devore 1982). The significance level of the actual correlation within the normal distribution was then determined. The two datasets (i.e., NCEP-2 and ERA-40) in Table 1 both show that the Niño-3.4 SST index and mean energy components (P_M and K_M) have the significant and maximal correlation when the lags are between 2 and 4 months, which implies that large-scale atmospheric processes respond to the SST anomalies during the El Niño and La Niña events with a time lag of ~2–4 months. The two datasets also show a significant correlation with a time lag of ~7 months between the Niño-3.4 SST index and the eddy kinetic energy K_E.

The perturbation of atmospheric temperature from its global mean controls the mean available potential energy. In addition, the zonal winds, which are related to the meridional gradient of atmospheric temperatures via the thermal wind relationship, are proportional to the mean kinetic energy. Therefore, the atmospheric

TABLE 1. Correlations (lag = 0) and maximum cross correlations between the Niño-3.4 SST indices and the global-average energy components. The numbers in parentheses denote significance levels. Positive (negative) lags correspond to the time series of energy components trailing (leading) the Niño-3.4 SST index.

	NCEP-2 (significance level)	ERA-40 (significance level)
Niño-3.4 index 1 (NOAA SST)		
Xcorr(Niño-3.4, P_M)	0.48 (1.2%), lag = 0	0.43 (1.3%), lag = 0
	0.51 (1.0%), lag = 2 months	0.52 (0.9%), lag = 3 months
Xcorr(Niño-3.4, K_M)	0.50 (1.1%), lag = 0	0.40 (1.3%), lag = 0
	0.67 (0.6%), lag = 3 months	0.59 (0.8%), lag = 4 months
Xcorr(Niño-3.4, P_E)	0.03 (40.5%), lag = 0	0.08 (18.9%), lag = 0
	0.08 (23.8%), lag = −2 months	0.10 (14.5%), lag = −1 months
Xcorr(Niño-3.4, K_E)	0.11 (20.7%), lag = 0	0.14 (17.8%), lag = 0
	0.37 (1.6%), lag = −7 months	0.39 (1.5%), lag = −7 months
Niño-3.4 index 2 (UCAR/CGD)		
Xcorr(Niño-3.4, P_M)	0.51 (1.0%), lag = 0	0.48 (1.0%), lag = 0
	0.54 (1.0%), lag = 2 months	0.58 (0.3%), lag = 3 months
Xcorr(Niño-3.4, K_M)	0.54 (1.0%), lag = 0	0.45 (1.1%), lag = 0
	0.69 (0.2%), lag = 3 months	0.64 (0.5%), lag = 4 months
Xcorr(Niño-3.4, P_E)	−0.001 (49.8%), lag = 0	0.05 (29%), lag = 0
	0.06 (27.4%), lag = −4 months	0.10 (19%), lag = −2 months
Xcorr(Niño-3.4, K_E)	0.07 (29.6%), lag = 0	0.1 (24.3%), lag = 0
	0.36 (1.0%), lag = −7 months	0.40 (1%), lag = −10 months

mean energies are closely related to the variation of atmospheric temperatures. Here we examine the correlation between the atmospheric temperature and SST in order to further investigate the relationship between the Niño-3.4 SST index (i.e., the SST anomaly) and the mean atmospheric energies in Fig. 1 and Table 1. Figure 2 displays the correlation between the two Niño-3.4 SST indices and the anomaly of the atmospheric temperature at 700 mb over the same area as the Niño-3.4 region (5°S–5°N, 170°–120°W). The 700-mb atmospheric temperatures correlate well with the SST anomaly. Figure 3 further displays the maximal cross correlation between the SST anomaly and the atmospheric temperature anomaly at different pressure levels over the Niño-3.4 area. The maximal cross correlation between the SST anomaly and lower atmospheric temperatures (i.e., 200–800 mb) is basically larger than 0.6 with a corresponding lag of ~2 months. The robust correlation between the SST anomaly and the lower atmospheric temperature explains the response of mean atmospheric energies (P_M and K_M) to the Niño-3.4 SST index in the El Niño and La Niña years. The eddy kinetic energy K_E is affected by the mean kinetic energy K_M (Peixoto and Oort 1974; Li et al. 2007), so the eddy kinetic energy K_E is related to the Niño-3.4 SST index (Table 1). It is possible that the conversion rates also affect the variation of energy components in the El Niño and La Niña years. However, the discrepancy estimates of the conversion rates between the two datasets prevent us from getting any robust conclusions.

We also conduct a quantitative investigation of the changed global atmospheric energies in the El Niño and La Niña years. We choose one whole year centered at the peak of the Niño-3.4 SST index (the magenta and green vertical dashed lines in Fig. 1) for five El Niño events (1982, 1987, 1991, 1995, and 1997) and three La Niña events (1988, 1998, and 1999) to compute the atmospheric energies in El Niño and La Niña events. Such a choice is based on two reasons: 1) a whole year can resolve seasonal variations in the atmospheric energetics (Li et al. 2007) and 2) a whole year is long enough to cover the response

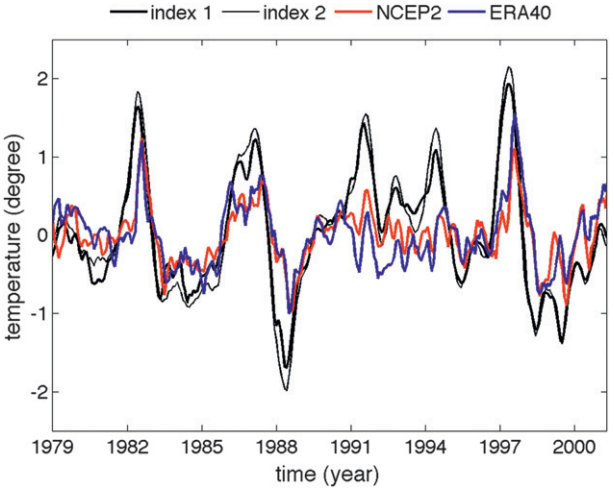

FIG. 2. Time series of the two Niño-3.4 SST indices and the anomaly of the 700-mb atmospheric temperatures over the Niño-3.4 area (5°S–5°N, 170°–120°W). The thick black line is for the Niño-3.4 SST index 1 and the thin black line is for the Niño-3.4 SST index 2. The red line and blue line are for the atmospheric temperature at 700 mb from NCEP-2 and ERA40, respectively.

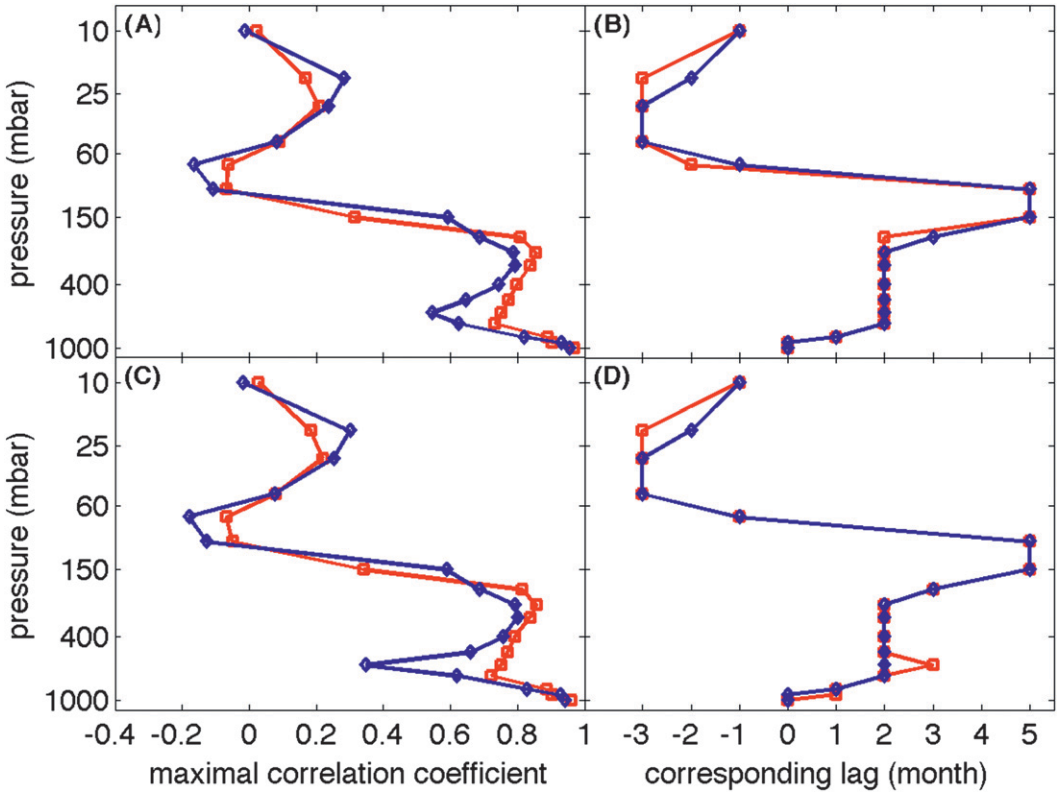

FIG. 3. (left) Maximal cross correlations and (right) the corresponding lags between the Niño-3.4 SST index and the atmospheric temperature anomaly at different pressure levels over the area of Niño-3.4. (a),(b) The correlations between the Niño-3.4 SST index 1 and atmospheric temperature from NCEP-2 (red line) and ERA-40 (blue line). (c),(d) As in (a),(b), but for the correlations between the Niño-3.4 SST index 2 and atmospheric temperature.

of atmospheric energetics to the oceanic signal with a time lag of ~2–4 months (Table 1). The atmospheric energies are averaged over all El Niño events and all La Niña events, respectively, to derive the atmospheric energetic in these warm and cold phases. Table 2 summarizes the difference of energy components between the El Niño/La Niña years and the normal years between 1979 and 2001. The two datasets (i.e., NCEP-2 and ERA-40) show consistent results of the changed mean energy components (P_M and K_M) in the El Niño/La Niña years. Compared with the normal years, the mean available potential energy P_M and the mean kinetic energy K_M in the El Niño years increase ~1%–2% and 3%, respectively. On the other hand, the mean available potential energy P_M and the mean kinetic energy K_M decrease ~2%–3% in the La Niña years. By examining the significance level, we find that the variation of mean energies is significant except for mean available potential energy P_M in the El Niño years from the dataset ERA-40. It is not clear why the variation of P_M in the El Niño years has different significances between the two datasets. Table 2 also shows that the eddy energies (P_E and K_E) increase in the El Niño years and decrease in the La Niña years except for the P_E in the La Niña years from NCEP-2 and the K_E

TABLE 2. Differences of the energy components between the El Niño/La Niña years and the normal years. The values shown in the table are the percentages of difference over the climatological values of energy components during the time period 1979–2001. The numbers in parentheses denote significance levels.

	El Niño (significance level)		La Niña (significance level)	
	NCEP-2	ERA-40	NCEP-2	ERA-40
P_M	1.5% (9%)	0.86% (43.9%)	−2.0% (6.7%)	−3% (2.5%)
K_M	3.2% (0.4%)	2.5% (3.1%)	−3.2% (1.6%)	−2.6% (6.6%)
P_E	0.6% (>55%)	0.07% (>55%)	0.94% (>55%)	−1.4% (48.1%)
K_E	0.02% (>55%)	−0.3% (>55%)	−0.75% (>55%)	−2.4% (9.9%)

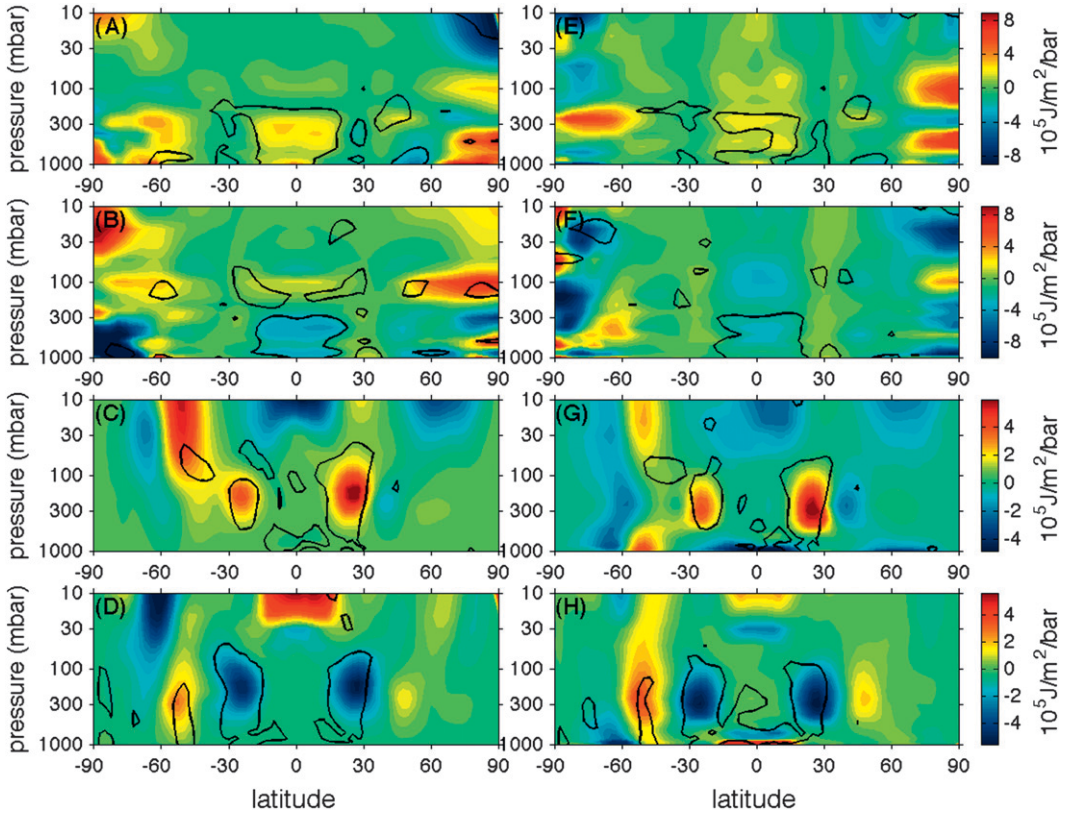

FIG. 4. Differences of the mean energy components (P_M and K_M) between the El Niño/La Niña years and the normal years in the latitude–altitude cross section. (a)–(d) The results based on NCEP-2 and (e)–(h) the results based on ERA-40. (a),(e) The difference of P_M between the El Niño years and the normal years. (b),(f) The difference of P_M between the La Niña years and the normal years. (c),(g) The difference of K_M between the El Niño years and the normal years. (d),(h) The difference of K_M between the La Niña years and the normal years. Differences that are statistically significant at or below the 5% significance levels are circled by black lines.

in the El Niño years from ERA-40. However, the differences for eddy energies (P_E and K_E) are relatively small and most values are not statistically significant.

In addition to examining the time series of global-average atmospheric energies, we explore the spatial patterns of the atmospheric energies in the El Niño and La Niña years. Figure 4 displays the difference of mean energy components (P_M and K_M) between the El Niño/La Niña years and the normal years in the latitude–altitude cross section. Areas circled by dark lines represent the differences with statistical significance at or below 5% significance level based on the Student's t test. The two datasets agree very well on the significant differences in the mean available potential energy P_M in the El Niño/La Niña years (Figs. 4a,b,e,f). Comparing the mean state of mean energies over the same 23-yr period (1978–2001; Li et al. 2007), we find that the varied P_M in the El Niño/La Niña years is concentrated in the equatorial region of the lower troposphere (300–1000 mb), which is a relatively weak maximum of P_M in the 23-yr mean state (Li et al. 2007). The varied atmospheric temperature gradients in the tropical regions, which correspond to the changed tropical SST in the El Niño and La Niña years, are responsible for the significant differences in the mean available potential energy. Figures 4c,d,g,h are the structures of differences in the mean kinetic energy K_M, which also display high agreement between the two datasets (NCEP-2 and ERA-40). These panels show that the significantly varied K_M in the El Niño/La Niña years are roughly in the same location as the maxima of K_M in the 23-yr mean state of energies (Li et al. 2007). The mean kinetic energy K_M is proportional to the squared velocity. The thermal wind relationship suggests that the temperature gradients in the meridional direction affect the mean zonal winds and further influence the mean kinetic energy. Therefore, the varied atmospheric temperature gradients in El Niño and La Niña years (Yuleava and Wallace 1994) also provide an explanation for the vertical structures of differences in the mean kinetic energy.

4. Conclusions

We conduct analyses of the mechanical energies of the global atmosphere in the El Niño and La Niña years based on the monthly evaluation of the two reanalysis datasets (NCEP-2 and ERA-40). Our analyses reveal significant correlations with a phase shift of ~2–4 months between the Niño-3.4 SST index and the mean energies of the global atmosphere. The general consistency between the two datasets further shows ~2% and ~4% increases in the El Niño years for the mean available potential energy and the mean kinetic energy, respectively. Our analysis also shows that the mean energies decreases ~2%–3% in the La Niña years. The exploration of the SST anomaly, the atmospheric temperature anomaly, and the atmospheric energies suggests that the variations of the mean energies in the El Niño and La Niña years are attributable to the changed atmospheric temperature gradients, which are driven by the tropical SST anomaly.

Acknowledgments. We thank M. Gerstell for helpful comments. This work was partly supported by the Jet Propulsion Laboratory, California Institute of Technology, under contract with the National Aeronautics and Space Administration (NASA). This work is also supported by NASA Outer Planets Research Program.

REFERENCES

Boer, G. J., and S. Lambert, 2008: The energy cycle in atmospheric models. *Climate Dyn.,* **30,** 371–390.

Devore, J. L., 1982: *Probability and Statistics for Engineering and the Sciences*. 1st ed. Brooks/Cole, 640 pp.

Goddard, L., and S. G. Philander, 2000: The energetics of El Niño and La Niña. *J. Climate,* **13,** 1496–1516.

Hirst, A. C., 1986: Unstable and damped equatorial modes in simple coupled ocean–atmospheric models. *J. Atmos. Sci.,* **43,** 606–630.

Hu, Q., Y. Tawaye, and S. Feng, 2004: Variations of the Northern Hemisphere atmospheric energetics: 1948–2000. *J. Climate,* **17,** 1975–1986.

Kanamitsu, M., W. Ebisuzaki, J. Woollen, S.-K. Yang, J. J. Hnilo, M. Fiorino, and G. L. Potter, 2002: NCEP-DOE AMIP-II reanalysis (R-2). *Bull. Amer. Meteor. Soc.,* **83,** 1631–1643.

Krueger, A. F., J. S. Winston, and D. A. Haines, 1965: Computation of atmospheric energy and its transformation for the Northern Hemisphere for a recent five-year period. *Mon. Wea. Rev.,* **93,** 227–238.

Li, L., A. P. Ingersoll, X. Jiang, D. Feldman, and Y. L. Yung, 2007: Lorenz energy cycle of the global atmosphere based on reanalysis datasets. *Geophys. Res. Lett.,* **34,** L16813, doi:10.1029/2007GL029985.

Lorenz, E. N., 1955: Available potential energy and the maintenance of the general circulation. *Tellus,* **7,** 157–167.

Margules, M., 1903: Uber die Energie der Sturme. *Jahrb. Zentralanst. Meteor.,* **40,** 1–26. (English translation by C. Abbe, 1910: *The Mechanics of the Earth's Atmosphere: A Collection of Translations.* No. 51, Smithsonian Institution, 553–595.)

Oort, A. H., 1964: On estimate of the atmospheric energy cycle. *Mon. Wea. Rev.,* **92,** 483–493.

——, and J. P. Peixoto, 1974: The annual cycle of the energetics of the atmosphere on a planetary scale. *J. Geophys. Res.,* **79,** 2705–2719.

——, and ——, 1976: On the variability of the atmospheric energy cycle within a 5-year period. *J. Geophys. Res.,* **81,** 3643–3659.

Peixoto, J. P., and A. H. Oort, 1974: The annual distribution of atmospheric energy on a planetary scale. *J. Geophys. Res.,* **79,** 2149–2159.

——, and ——, 1992: *Physics of Climate*. American Institute of Physics, 520 pp.

Phillips, N. A., 1956: The general circulation of the atmosphere: A numerical experiment. *Quart. J. Roy. Meteor. Soc.,* **82,** 123–164.

Press, W., S. Teukolsky, W. Vetterling, and B. Flannery, 1992: *Numerical Recipes in Fortran 77: The Art of Scientific Computing*. 2nd ed. Cambridge University Press, 933 pp.

Rayner, N. A., D. E. Parker, E. B. Horton, C. K. Folland, L. V. Alexander, D. P. Rowell, E. C. Kent, and A. Kaplan, 2003: Global analyses of sea surface temperature, sea ice, and night marine air temperature since the late nineteenth century. *J. Geophys. Res.,* **108,** 4407, doi:10.1029/2002JD002670.

Sheng, J., and Y. Hayashi, 1990: Observed and simulated energy cycles in the frequency domain. *J. Atmos. Sci.,* **47,** 1243–1254.

Smith, T. M., R. W. Reynolds, T. C. Peterson, and J. Lawrimore, 2008: Improvements to NOAA's historical merged land–ocean surface temperature analysis (1880–2006). *J. Climate,* **21,** 2283–2296.

Steinheimer, M., M. Hantel, and P. Bechtold, 2008: Convection in Lorenz's global energy cycle with the ECMWF model. *Tellus,* **60,** 1001–1022.

Trenberth, K. E., 1997: The definition of El Niño. *Bull. Amer. Meteor. Soc.,* **78,** 2771–2777.

Uppala, S. M., and Coauthors, 2005: The ERA-40 re-analysis. *Quart. J. Roy. Meteor. Soc.,* **131,** 2961–3012.

Wiin-Nielsen, A., 1959: A study of energy conversion and meridional circulation for the large-scale motion in the atmosphere. *Mon. Wea. Rev.,* **87,** 319–332.

Yamagata, T., 1985: Stability of a simple air-sea coupled model in the tropic. *Couple Ocean–Atmospheric Models,* J. Nihoul, Ed., Elsevier Oceanography Series, Vol. 40, Elsevier, 637–657.

Yulaeva, E., and J. M. Wallace, 1994: The signature of ENSO in global temperature and prediction fields derived from the microwave sounding unit. *J. Climate,* **7,** 1719–1736.